# NIOBIAN RUTILE AND ITS ASSOCIATIONS AT JOLOTCA, DITRAU ALKALINE INTRUSIVE MASSIF, EAST CARPATHIANS, ROMANIA

Paulina HIRTOPANU[1], Robert J. FAIRHURST[2] and Gyula JAKAB[3]

[1]Department of Mineralogy, University of Bucharest, 1, Nicolae Balcescu Blv., 010041 Bucharest, RO;
[2]Technical Laboratory at Lhoist North America, Inc., 3700 Hulen Street, Forth Worth, Texas 76107, US;
[3]IG Mineral Gheorgheni, Romania
*Corresponding author*: Paulina HIRTOPANU, E-mail: paulinahirtopanu@hotmail.com

The Nb-rutile at Jolotca, situated in Ditrau alkaline intrusive complex occurs as intergrowths with ilmenite, Mn-ilmenite, Fe-pyrophanite and has ferrocolumbite, manganocolumbite, aeshynite-(Ce), aeshynite-(Nd), fergusonite-(Y), euxenite-(Y) and polycrase-(Y) exsolutions. The textural relations in this association show the replacement of niobian rutile by ilmenite and Mn ilmenite. Niobian rutile is the oldest mineral. Ilmenite and Mn-ilmenite occur as lamellar exsolutions in niobian rutile and as veins, and separately, in grains as solid solution with Fe-pyrophanite. The range of $Nb_2O_5$ content in Nb rutile varies generally from 2 to 15% wt. Sometimes, the values of $Nb_2O_5$ (up to 37.5% wt) are higher than any previously recorded for rutile from alkaline suites, pegmatites and carbonatites, having a chemical composition similar to that of old name „ilmenorutile". Because of such a big difference in chemical composition, and the different kind of appearances of the two rutiles, they can be separated into two Nb rutile generations. The first niobian rutile (niobian rutile I) formed on old rutile, has low $Nb_2O_5$ (10-15wt%), and oscillatory composition. Its composition is characteristically close to stoichiometric $TiO_2$. The Nb-rutile II, less widespread, has no zonations, has a smooth surface and it is Nb-richer than early Nb rutile I. Some low $Cr_2O_3$ content of Jolotca Nb-rutile and low Ta concentrations indicate a relatively high-pressure regime of its genesis (Tollo & Haggerty). The occurrence of niobian rutiles could be linked with a carbonatite (?)/alkaline phase of the alkaline intrusive Ditrău complex. The presence of $Cr_2O_3$ in its composition suggests a mantle origin. It is difficult to establish the possible precursors of such ilmenite-rutile intergrowths and their Nb, REE(Y) mineral suite exsolutions. The mineralizing process was multi-staged which was supported by textural relationships, where there are replacements of earlier rutile, by Nb rutile I, then the appearance of richer Nb rutile II. The last stage could be the appeareances of Mn-columbite/Fe-columbite, yttrocolumbite-(Y), aeshynite-(Ce), aeshynite-(Nd), polycrase-(Y) and euxenite-(Y) as exsolutions in niobian rutile/ilmenite intergrowth, from a common solid solution. The original precursor product from the upper mantle was probably a mixture linked by a high pressure crystalographically sheard rutile structure (Tollo & Haggerty, 1987). When the temperature and pressure fall, these compounds from the original mixture become unstable and their exsolutions occur.

*Key words*: Nb rutile, ilmenite, rich niobian rutile, Mn-ilmenite, Mn/Fe-columbites, yttrocolumbite-(Y), aeshynite-(Ce), aeshynite-(Nd), euxenite-(Y), polycrase-(Y), exsolutions, high Tand P progenitors, upper mantle.

## INTRODUCTION

Several oxide minerals (cassiterite, rutile, ilmenite and wolframite) incorporate minor to substantial quantities of Nb and/or Ta into their structures that substitute mainly for $Sn^{4+}$, $Ti^{4-}$ or $W^6$. These substitutions are largely coupled with the charge-balancing entry of Fe, Mn or Sc (Černý and Ercit, 1989). In Nb-Ta bearing geochemical environments, rutile readily accepts Nb and Ta into its structure, mainly in tapiolitelike stoichiometry with Fe>Mn. The rutile incorporates a tapiolite component by substituting $(Fe,Mn)^{2+}+2(Ta,Nb)^{5+}$ for $3Ti^{4+}$. The substitution of the $Ti^{4+}\leftrightarrow2Fe^{2+}$ can

happened in the niobian rutile of Jolotca, at the same time with Nb incorporation and when the iron content increases over Mn. Niobian rutile has been known for 150 years mainly under its currently varietal name „ilmenorutile". However, it does not represent a distinct mineral species as it is only a (Fe,Nb)- enriched but still Ti dominant derivative rutile (Černý *et al*., 2007). These last authors consider that niobian rutile is in most cases exsolved into a (Fe,Nb)- depleted rutile+titanian ferrocolumbite or titanian ixiolite. Relics of the original homogeneous phase are scarce and largely only microscopic in size (Černý *et al*., 2007). Intergrowths of ilmenite and rutile have been reported from a number of kimberlite localities in recent years. The mode of origin most commonly proposed for such ilmenite-rutile intergrowth involves the high pressure breakdown of a precursor pseudobrookite-type phase similar to armalcolite $(Fe, Mg)Ti_2O_5$ in composition (Tollo & Haggerty, 1987). The composition of rutile in these intergrowths, however, differs markedly from stoichiometric $TiO_2$; combined $Cr_2O_3+Nb_2O_5$, sometimes and $ZrO_2$ contents, may be as large as 29% wt, making armalcolite an unlikely candidate as a precursor phase (Tollo & Haggerty, 1987). An alternative proposal is replacement of rutile by ilmenite (Pasteris, 1980). In general, the rutile from granites and granitic pegmatite complexes is characterized by a lower Nb/Ta value and may be contrasted with the relatively Nb-enriched carbonatitic rutile. Kimberlitic rutile shows considerable enrichment in niobium, limited substitution of iron, and only a slight amount of tantalum (Tollo & Haggerty, 1987). The rutile from alkaline igneous suites appears to be characterized by a greater extent of substitution of both iron and tantalum, and by lower concentrations of niobium. The rutile from carbonatitic complexes tends to cluster closer to the Nb-Fe sideline, than the rutile from granitic pegmatites, which characteristically show a greater extent of Ta substitution (Tollo & Haggerty, 1987). Judging from this point of view, the Jolotca Nb rutile is similar with that from alkaline/carbonatite complexes, because of its high Nb, Fe, Mn (Fe<Mn) contents, low Ta content and some $Cr_2O_3$ content.

The electron microprobe data, that we present below, were collected on a JEOL8200 instrument located at the Camborne School of Mines, University of Exeter, Cornwall, UK. Images and chemical analyses were collected using an accelerating voltage of 15KeV and 30nA beam current. X-ray spectra were collected using EDS and WDS detectors calibrated with natural and synthetic standards. There were realized many backscattered electron images (BSEi), helping us to establish textural relationships, fine scale intergrowth of the niobian rutile, ilmenites, columbites, aeshynites and euxenites, illustrated in the text. Also, the Nb rutile oscillatory/zoned compositions, can be seen in many optical and electronic images.

## GENERAL PETROGRAPHY AND MINERALOGY OF DITRAU ALKALINE INTRUSIVE COMPLEX

The Ditrau alkaline intrusive complex is situated within the crystalline rocks of the inner part of the East Carpathians, Romania. It has a distinct ring structure and a succession of magmatic events ranging from gabbroic and dioritic magma to syenitic and various postmagmatic events as well, all developed between a Triassic extensional stage and a Jurassic rifting stage (Krautner & Bindea, 1995). The succession of magmatic events in Ditrau could be completed with carbonatite intrusion (?), that followed after the alkaline intrusion and used the same pathways of the previous alkaline silicate melt. Its affiliation to anorogenic alkaline magmas explains their general feature Nb>>Ta and the predominance of LREE over HREE. The Ditrau alkaline intrusive complex represents the end of long lasting fractionation processes in the crust and deep upper mantle, respectively. This explains the modest dimensions of Ditrau intrusion and its enrichment with incompatible elements. The Ditrau intrusion appears to be the product of open system crystallization at low temperatures and low pressures of a chlorine-enriched agpaitic magma. Maybe the parental magma is itself a late stage derivative magma of a more fundamental melt that had existed at a depth from which were derived the major current nepheline syenite complex.

The main petrographic mineralogical rock groups of Ditrau massif are: peridotites and gabbroids rocks, hornblendite, melanodiorite, diorites, monzonite and monzodiorite, syenites,

nepheline syenite, quartz syenites, granites and lamprophyres (Fig. 1). In the Jolotca mineralizing area the main petrographic type rocks belong to ultrabazites and basites/hornblendites, with gradual transition toward diorites, diorites monzonites and monzonites. This petrographic complex is penetrated by non filonian syenites and filonian lamprophyres. The Jolotca mineralizations has a predominant vein character (Fig. 2). The veins are displayed as simple and subparalel groups, with the E-W orientation and the north falls of 40–60°. Often the veins are accompanied by impregnations, nests and networks of little veins mineralization. The veins have a length of around a few hundred meters up to 1kilometre, a width between 5– 150 cm and sometimes could reach 20 m, and a depth of 650 m. Among them, the Filip-Simo and Toth Vesze veins have the higher ilmenite-rutile association content.

The mineralizing veins are situated predominantly in the hornblendite and diorite areas (Fig. 2). Very rarely here were observed some mineralizing veins in syenites, monzonites or granites. No genetic affiliation has been observed between mineralizing veins and host rocks, represented by hornblendites and diorite. The mineralogical composition of the veins is extreme variable, but the main components are sulphides, the REE and Nb-Ta-Ti-Fe minerals. Some sulphides occurring in Jolotca veins are: pyrite, marcasite, galena, sphalerite, chalcopyrite, arsenopyrite, pyrrhotite, joseite, matildite-schapbachite, molibdenite, valleriite-mackinawite, cubanite, safflorite, bornite, tetrahedrite, etc. The magnetite is associated to sulphides. The intergrowth niobian rutile+ilmenite occurs as nests/ nodules of some cm in size, in the association spalerite /pyrite-calcite (Fig. 3), and sometimes with pyrite-monazite and REE-carbonates. Generally, the intergrowth ilmenite-Nb rutile nodules represent around 3% from all mineralizing vein in the Filip Simo vein, and much higher in the Toth Vesze vein (around 6–7%). The Ditrau alkaline massif has a complexity and a great diversity of mineral occurrences (Jakab, 1998; Constantinescu, 1999; Hirtopanu *et al*., 2010a, 2010b, 2013a, 2013b; Molnar, 2010).

The rare element minerals which were determined in Ditrau/Jolotca veins belong to the following classes (in the predominant order) (Hirtopanu *et al*., 2010a): **I. LREE(Y)-carbonates**: bastnaesite-(Ce), bastnaesite-(La), parisite-(Ce), parisite-(La), synchysite-(Ce), kainosite-(Y), thor-bastnaesite, REE-Fe-Ca carbonate; **II. Oxide** minerals of Nb, Ta, REE(Y), Ti, Fe: 1. Columbite-Tantalite group: ferrocolumbite, mangancolumbite, yttrocolumbite; 2. Aeschynite group: Aeschynite-(Nd), aeschynite-(Ce), aeschynite-(Y); 3. Euxenites: euxenite-(Y), polycrase-(Y); 4. Niobian rutile; 5. Secondary Th, Ce, U oxides: thorianite, cerianite-(Ce), uraninite; **III. REE(Y)-phosphates**: REE-apatite, REE-carbonate -fluorapatite, monazite-(Ce), brabantite-huttonite and huttonite-monazite series, cheralite, brockite, xenotime-(Y), karnasurtite-(Ce) (?); **IV. REE-(Y)-Th-Zr Silicates**: allanite-(Ce), thorite, thorogummite (Fe-thorogummite, Fe-Zr-thorogummite, Pb-thorogummite), cerite-(Ce), lessingite-(Ce), törnebohmite-(Ce), Th-zircon, chevkinite-(Ce), cerite-(Ce), stillwellite-(Ce) and tritomite-(Ce); **V. Halides**: Y-fluorite, fluorite; **VI. Tellurides**: Bi-Te (hedleyite) and unnamed Bi, Pb-Te.

The Jolotca vein type rare element mineralisation rich in LREE, Nb, Ti, Fe, and sulphides differs from Belcina mineralization types area with Y and Th mineralization, less LREE, less sulphides and rich in Fe-oxides and hydroxides and diverse carbonates, situated outside the massif (towards SE), in the surrounding metamorphic rocks of Tulghes Group (Hirtopanu, 2013b). The Belcina occurrence is mostly constituted of intergrowths of Th silicates and Y-phosphates [(thorite, thorogummite and xenotime-(Y)] and other like zircon, less niobian rutile, ferrocolumbite, Y-fluorite, less sulphides, and almost no Nb-Ta pyrochlores (which occur in Jolotca area), almost no REE(Y)–silicates (allanite, chevkinite, which has a big development in Jolotca area), and almost no REE(Y)-carbonates (which also have a big development in Jolotca area) (Hirtopanu *et al*., 2013b). The biggest Jolotca occurrence from the NW of the massif is of vein type and comprises a complex sulphide mineralization and complex Ti-Nb-Fe-Mn oxides. The last one is studied in this work. The rare elements mineralizations appear to be earlier than associated sulphides-magnetite, almost all the rare element minerals being cut by sulphide veins. The Jolotca vein mineralisation has a gangue of ferrodolomite, ankerite, siderite and calcite.
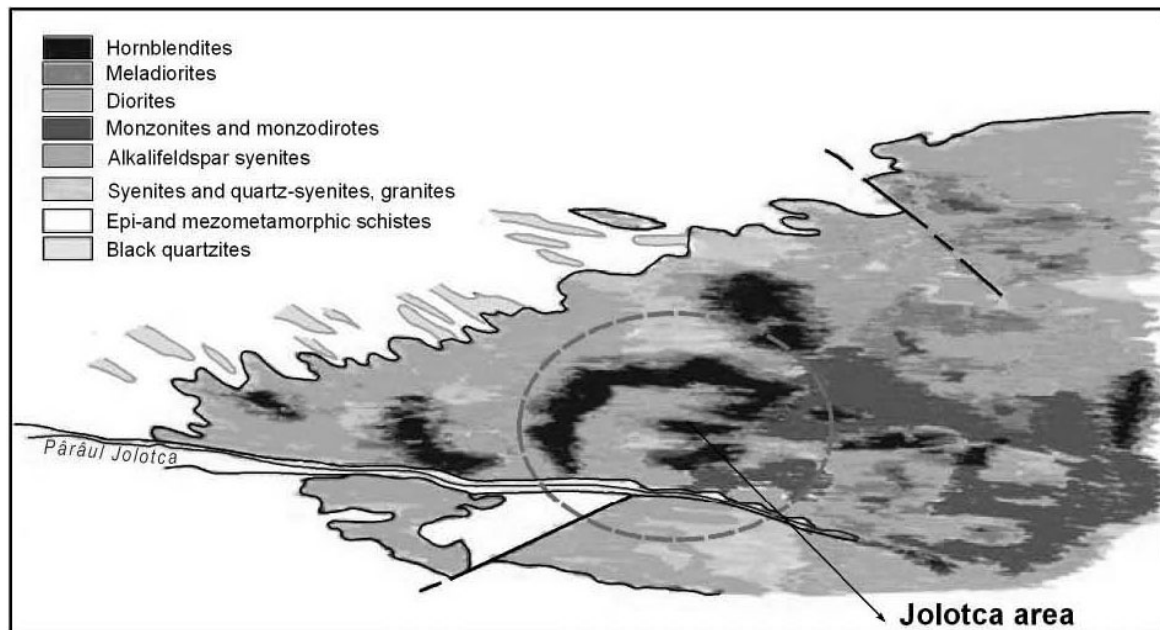
Fig. 1. The schematic petrographic map of a part of the Ditrau alkaline massif (Jakab, 2014).
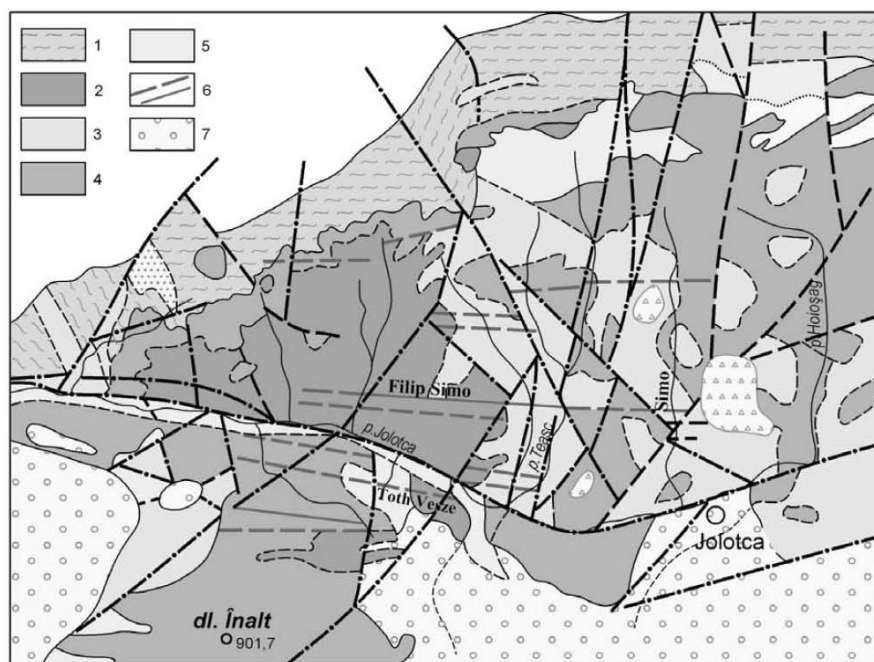See the enlargement of Jolotca area in Figure 2.



Fig. 2. Jolotca area with mineralizing vein field: 1. Metamorphic rocks; 2. Hornblendite; 3. Diorite; 4. Syenite;
5. Monzonite; 6. Mineralizing veins; 7. Quaternary deposit (Jakab, 2014).

## NIOBIAN RUTILE, OPTICAL PROPERTIES AND CHEMISTRY

**Niobian rutile** $(Nb,Ti)O_2$, occurs as main constituent mineral in Nb-Fe-Mn-REE oxide association. The coarse grains of niobian rutile (more than a few cm) occur in the calcite mass associated with REE carbonate, monazite-(Ce) and diverse sulphides, especially sphalerite. Nb-rutile is tightly intergrown with ilmenite, manganilmenite and niobian ilmenite. Macroscopically Nb-rutile has a black bright to steel-grey colour, occurring as round to ovoid nodules/veins of a few cm and bigger in calcite while the ilmenite is black.
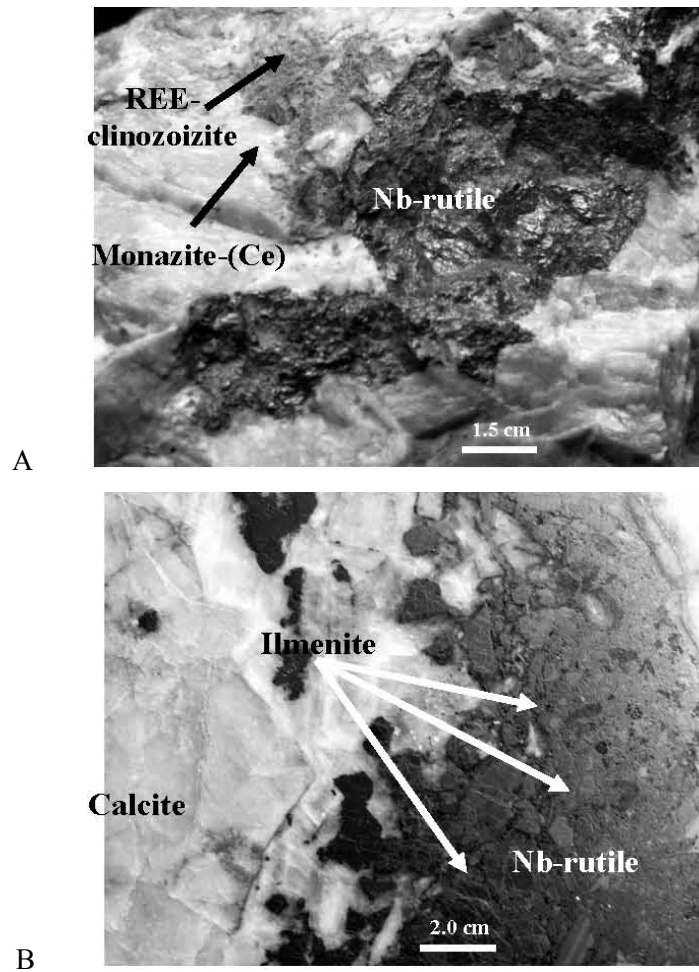
Fig. 2. A. Niobian rutile (grey) in calcite (white), monazite-(Ce)(red), REE-clinozoizite (green), sample Dt214 (left):
see its BSE image in Figure 9; B. Niobian rutile (grey) intergrown with ilmenite (black), sample 2006/13 (right).
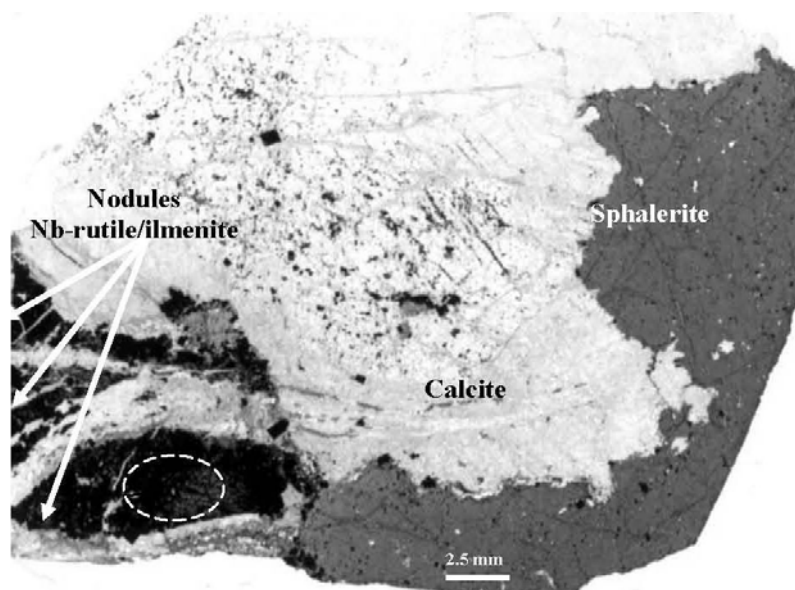Both samples were collected from Toth Vesze vein.



Fig. 3. Photomicrograph of sample Dt11, plane polarized light: nodules of Nb rutile (brown black, left bottom corner)
intergrown with Mn-ilmenite (black), sphalerite (yellowish light brown), calcite (light grey/white).
See the optical images of intergrowths of Nb-rutile with Mn-ilmenite in Figure 4, out of white circle.
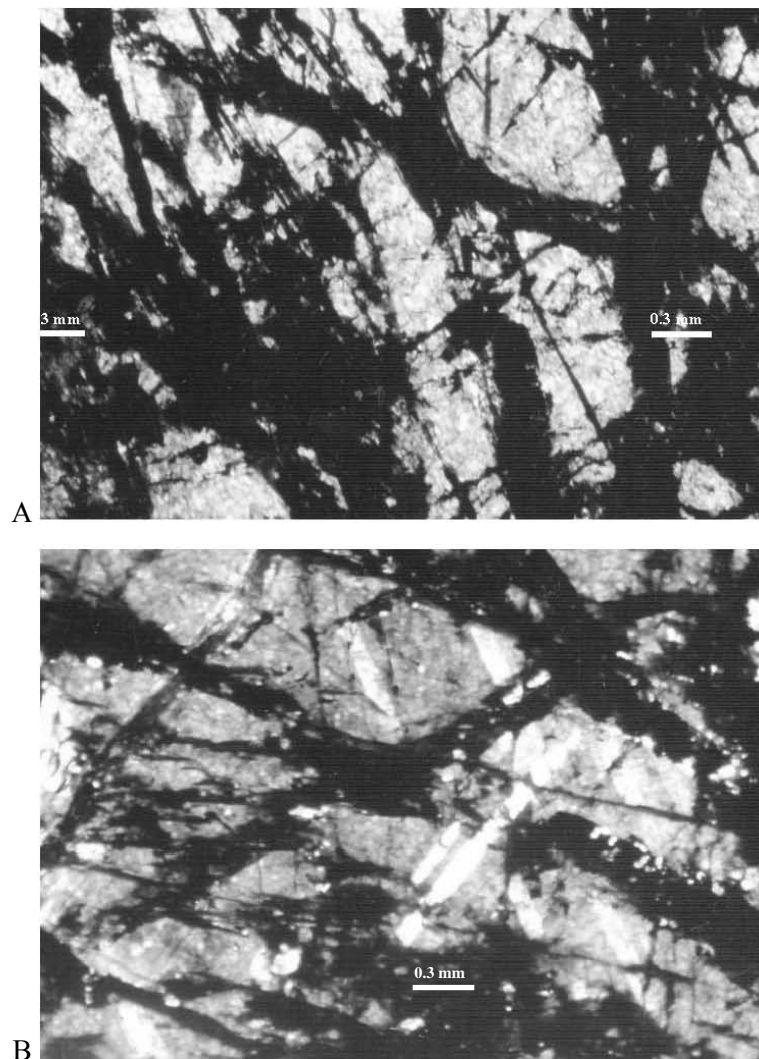
Fig. 4. Niobian rutile (yellow grey, white), Mn-ilmenite (black), NII (A photo) and N+ (B photo), sample Dt11; these images are enlarged from Fig. 3, out of white circle.

This high niobian-containing variety of rutile is similar with that of old name „ilmenorutile". The „**ilmenorutile**" $(Nb,Fe,Ti)O_2$, was discredited by an IMA procedure (Burke, 2006). The $Nb_2O_5$ content of „ilmenorutile", previously described (Hirtopanu, 2010), has general variations between 25–35% and sometimes even more (Table 2), over the $TiO_2$ content, being much higher than that of early niobian rutile. It could be another niobian rutile generation, named rich niobian rutile or rutile II, and has probably a ilmenite structure (?). In the photomicrograph of sample Dt11 (from Toth Vesze vein) in Figure 3 one can see some short lenses/nodules of Nb rutile intergrown with ilmenite embedded in calcite. They seem to be earlier than the yellow sphalerite which cuts these brown black short lenses. In transmitted light one can see how the niobian rutile is intersected by many Mn-ilmenite veins (Fig. 4). In the intergrowth of ilmenite/rutile, in reflected/ tramsmitted light, the ilmenite occurs in two distinct modes: the lamellar (Fig. 11 left) inside the rutile host, and ilmenite could be rimmed these intergrowths (Fig 12 left). The rim and lamellae ilmenite sometimes are continuous, with individual lamellae branching into the interior from the periphery (Fig. 12, left).

In the photomicrograph of polished thin section in Figure 3 the Nb-rutile has yellow-black colour. In transmitted light, in NII, niobian rutile has a brown, brown violet to yellow green, yellow reddish, yellow colour with great pleochroism and complex zonations (Figs. 5–8). The zonation composition of Nb rutile can also be seen in its back scattered electron (BSE) images in Figs. 9 and 10. The substitution in niobian rutile and ilmenite is due to the isomorphism of $Ti^{4+}$ with $Nb^{5+}$ and $Fe^{2+}$, and goes probably after the schemes: $2Ti^{4+} \leftarrow Nb^{5+} + (Fe,Al)^{3+}$;

$3Ti^{4+}\leftarrow 2Nb^{5+}+Fe^{2+}$; $3Ti^{4}\leftarrow(Fe,Mn)^{2+}+2(Ta,Nb)^{5+}$ (Černý, 1999). The grains of Jolotca niobian rutile show omnipresent oscillatory zoning because of fluctuations in the activity of the components involved in the parental medium, represented very well in the BSE image in Figs. 9 and 10. The content of $Nb_2O_5$ predominates over $Ta_2O_5$. The range of $Nb_2O_5$ vary generally between 2–15% wt, for earlier niobian rutile I. The $Ta_2O_5$ content is very low, practically this Nb rutile has no tantalum. Also, the content of FeO (1–15.00%wt) is much higher than that of MnO (0–0.1%wt). Some low $Cr_2O_3$ contents (1.48%wt) in niobian rutile were determined in the samples DT214R and Dt2013/in Jolotca area (Table 1). The $Cr_2O_3$ content is characteristic for niobian rutile and ilmenite in the Orapa kimberlite, Botswana, originated from the upper mantle (Tollo & Haggerty, 1987).



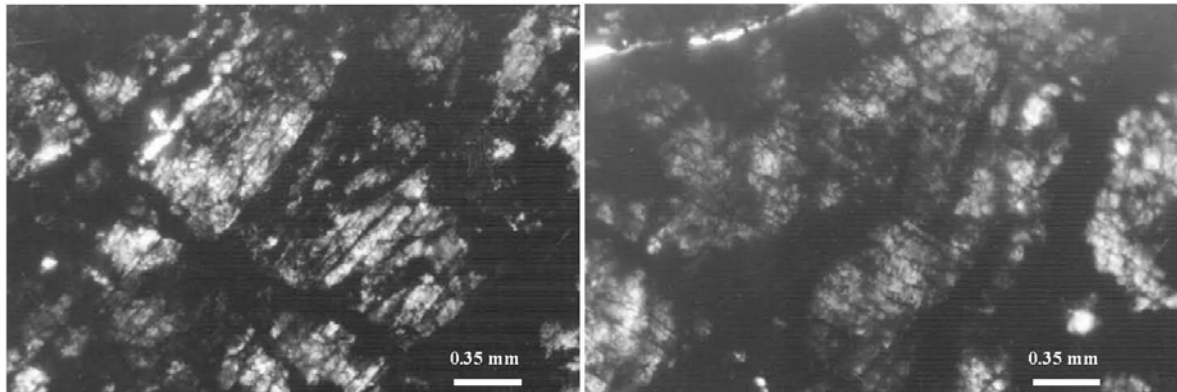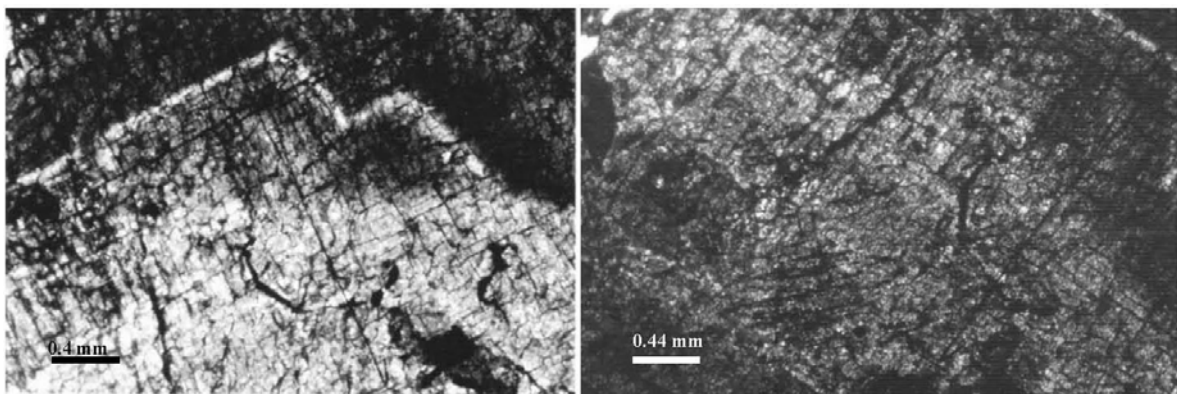Fig. 5. Pleochcroism in Nb rutile: white, yellow, red yellow, violet, yellow-brown, brown NII, sample Dt 212.



Fig. 6. Optical images of Nb rutile with $Cr_2O_3$: cleavages and zonation, transmitted light, N+, sample Dt214R (left) and Dt2006/13 (right). See its microprobe composition in Table 3.
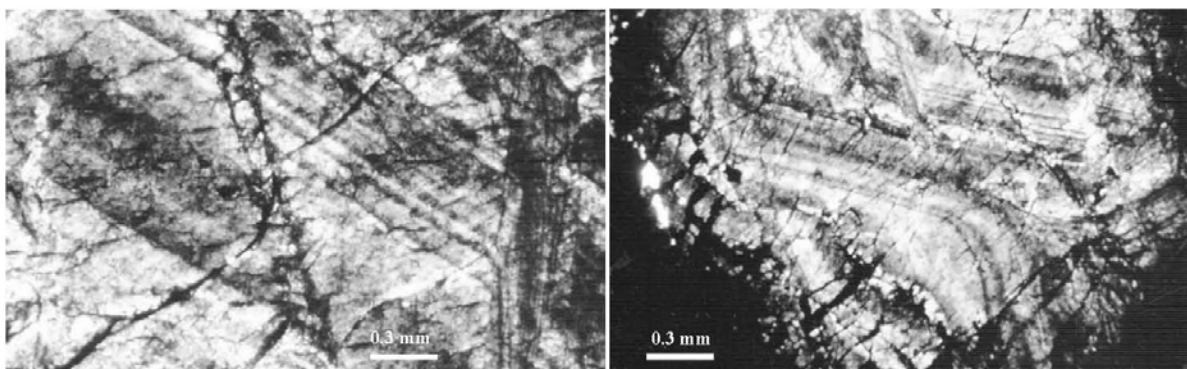


Fig. 7. Zonations in Nb rutile: more Nb, yellow brown and less Nb, light yellow, NII, sample Dt214; See its BSE image in Figure 9.
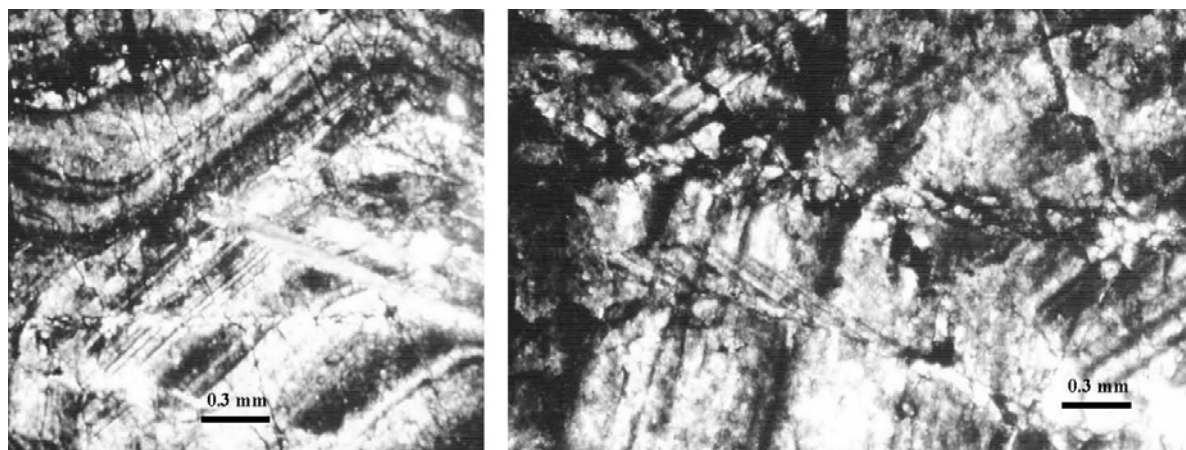
Fig. 8. Zonation and pleochcroism in niobian rutile, sample Dt214; see its BSE image in Figure 9.

*Table 1*

The microprobe composition of rutile niobian with $Cr_2O_3$, samples Dt214R and Dt2006/13a;
see their optical images in Figure 6

| Samples | Dt214R | Dt2007/13a |
|---------|--------|------------|
| $TiO_2$ | 87.62 | 87.10 |
| $Cr_2O_3$ | 1.47 | 1.34 |
| $Nb_2O_5$ | 10.89 | 10.65 |
| Total | 100.00 | 99.107 |

The zonations are a greatly predominant feature of the Jolotca primary niobian rutile. Variation in Nb and Ta, individually as well as collectively control the gross oscillatory patterns and are opposite to Ti (Černý *et al.*, 2007). Because the Jolotca niobian rutile has no Ta, the zonation is a result of Nb, Ti, Fe, Mn and $Cr_2O_3$ variations. A narrow zone of low level Nb (dark grey) is followed by a broader zone of slightly increased substitution (medium grey) and an even broader zone with high concentration of this element (Figs. 9, 10). The fluctuations would have to be synchronized among at least four cations: $Fe^{2+}$, $Mn^{2+}$, $Nb^{5+}$ and $Ta^{5+}$. These last authors consider that the difference in diffusion rates of different cations at the boundary layer of the parent medium along the growth surfaces of niobian rutile can be expected. Most of Nb, Ta, W and Fe plus a host of minor elements are exsolved. In the Jolotca niobian rutile, the form of columbite-like phase occurs on cooling. The exsolution products in niobian rutile are controlled by the (Fe+Mn+Sc)/(Nb+Ta+W) ratio of the primary phase and by its $(Fe^{3+}+Sc)/(Fe^{2+}+Mn)$ ratio (Černý *et al.*, 1999). Dominance of the divalent A-cations facilitates exsolution of titanian ferro- to mangano- columbite, or titanian ixiolite, whereas dominant trivalent cations lead to exsolution of titanian $(FeSc)^{3+}NbO_4$ phases. Excess (Fe,Mn) over the columbite-type $Fe^{2+}Nb$ stoichiometry causes exsolution of (Fe,Mn)-rich Nb-Ta-oxide minerals or complementary (Fe,Mn,Ti) phases (Černý *et al.*, 1999).

Chemical compositions determined by electron microprobe analyses for coexisting ilmenite and rutile from individual nodules are presented in Table 2. The host rutile of the intergrowths shows a broad range of compositional variation and is typically characterized by significant substitution of niobium (2.80–9.34 wt% $Nb_2O_5$). Iron is generally present in low concentrations. The FeO contents (as total iron) varies in the range of 1.22–4.27 wt.%. The Ditrau niobian rutile shows very low Ta content. Generally, the Jolotca niobian rutile shows enrichment in niobium, limited substitution of iron and only a very slight amount of tantalum (0–0.06 wt.%). All the Fe is determined as $Fe^{2+}$. The $Fe_2O_3$ was not calculated. Compositions containing substantial $Fe^{3+}$ are well documented by many researchers and the rutile type compound $Fe^{3+}NbO_4$ could be incorporated in Jolotca Nb-rutile composition. Also, in the future, the presence of $Ti^{3+}$ and $Ti^{2+}$, induced by the entrance of $Fe^{3+}$ and $Fe^{2+}$, needs to be determined. The MnO content of niobian rutile I is under 1% wt, whereas the niobian rutile II has 10–14%. The MgO content, although very low, shows that the

Mg is present in niobian rutile II composition. TheTiO$_2$ content is lower than in niobian rutile I, being similar to that of old name ilmenorutile. The Dy$_2$O$_3$ contents in niobian rutile II are also present in old niobian ilmenite as well. The niobian rutile II occurs in close association with niobian rutile I, ilmenite, ferrocolumbite, manganocolumbite, aeschynite-(Nd), aeschynite-(Ce), allanite-(Ce), chevkinite-(Ce). The mangancolumbite forms exsolutions in niobian rutil II as it does in niobian rutile I (Fig. 10). Also, some grains of niobian rutile that occur separately, not in intergrowth with ilmenite, have been analysed by electronic microprobe and their compositional data are shown in Tables 3, 3A, 3B.
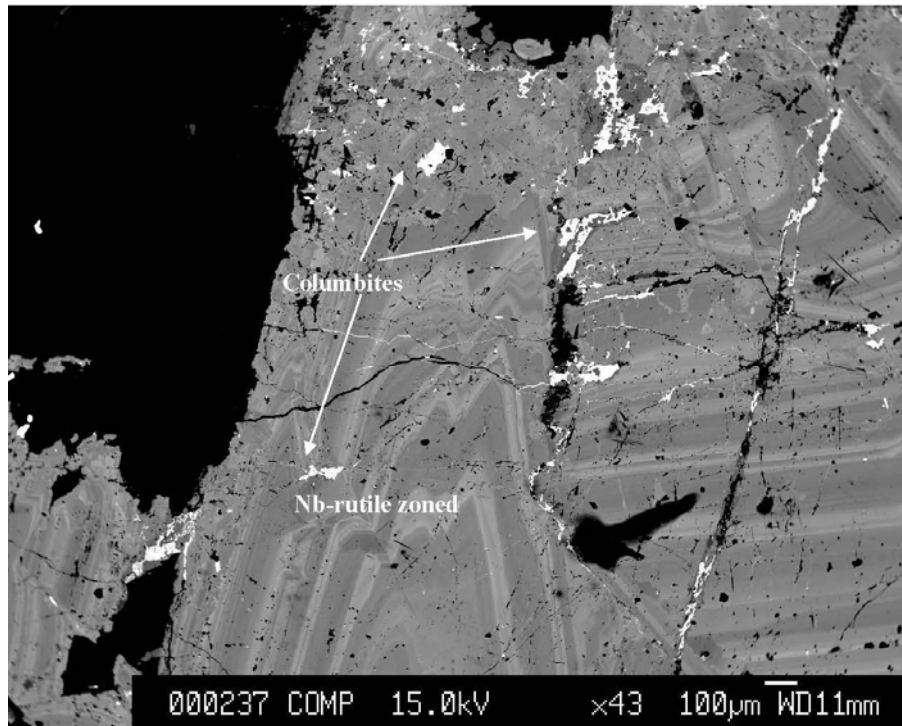


Fig. 9. Back scattered electron (BSE) image of zoned Nb rutile: more Nb (light), less Nb (grey); ferrocolumbite /manganocolumbite+euxenite-(Y) (white, veinlets, nests), calcite (black), sample Dt214.
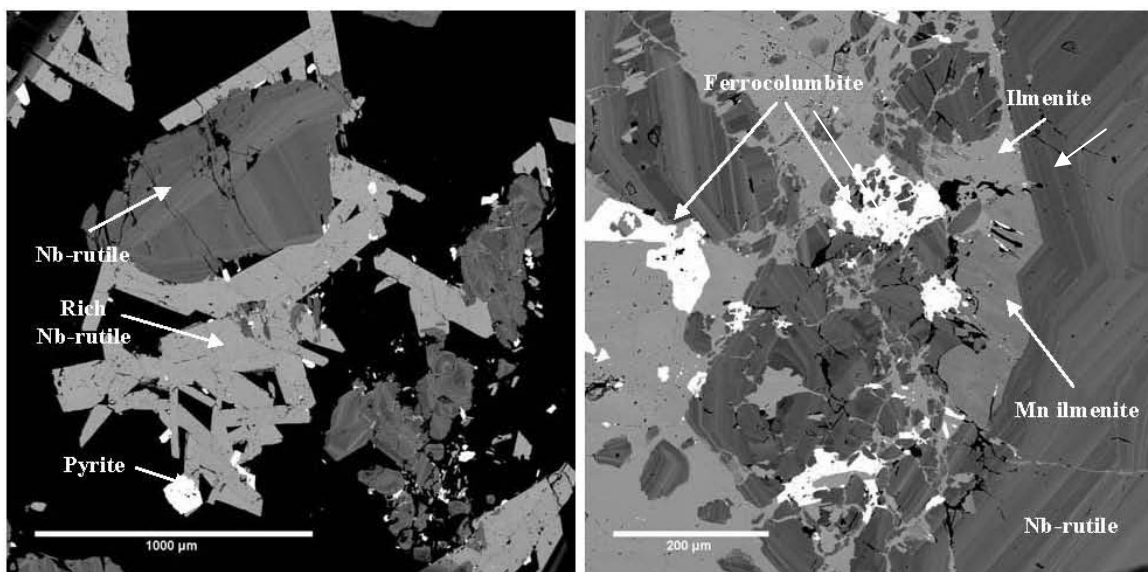


Fig. 10. Back scattered electron (BSE) image of Nb-rutile (dark grey, zoned, less Nb), rich Nb-rutile (light grey prisms); see their composition in Tables 3B and 4, respectively; Mn- and Fe- columbites (small, white), pyrite (big, white, bottom), sample Dt214R/4 (left image); Nb rutile (grey, zoned), ilmenite (light grey, smooth), manganilmenite (dark grey lamellar intergrowth/unmixed with/in ilmenite), ferrocolumbite (white), sample Dt214R/3 (right image). (Hirtopanu *et al*., 2010a).

Fig. 11. Back scattered electronic (BSE) image of niobian rutile (light grey), manganese ilmenite (lamellar, dark grey), mangancolumbite (white), sample 2006/13 (left image); BSE image of rutile (centre, grey dark), Nb rutile (light grey, around rutile, with zoned composition), ferrocolumbite (very small, inside niobian rutile), thorite (white/light grey, with oscillatory composition, outside niobian rutile), quartz (black), sample Bel10A/4A (right image) (Hirtopanu *et al.*, 2013b).

*Table 2*

Microprobe analysis of intergrowths Nb-rutile and ilmenite; sample 2006/13: point 1, 2=Nb rutil, 4, 5 = Mn ilmenite; 13=Nb rutile, 14=Mn ilmenite; 15, 16=Mn ilmenorutile, rich Nb; Dt39: 20 = Mn-ilmenite, 23, 24 = Nb rutile

|  | 1 | 4 | 2 | 5 | 13 | 14 | 15 | 16 | 20 | 23 | 24 |
|---|---|---|---|---|---|---|---|---|---|---|---|
|  | Nb-rutile/Mn-ilmenite | | Nb-rutile/Mn-ilmenite | | Nb-rutile /Mn-ilmenite | | Mn-ilmenorutil | | Mn-ilmenite/Nb rutile | | |
| $Y_2O_3$ | 0 | 0 | 0 | 0 | 0 | 0 | 0 | 0.05 | 0 | 0 | 0 |
| $Ta_2O_3$ | 0 | 0 | 0 | 0 | 0.06 | 0 | 0.04 | 0.03 | 0.03 | 0 | 0 |
| $ZrO_2$ | 0 | 0 | 0.01 | 0 | 0 | 0 | 0 | 0.03 | 0.01 | 0.02 | 0.01 |
| $SiO_2$ | 0.02 | 0.01 | 0.05 | 0 | 0.01 | 0 | 1.99 | 0.03 | 0.10 | 0 | 0 |
| $Nb_2O_5$ | 2.80 | 1.80 | 9.34 | 3.60 | 8.03 | 1.48 | 24.69 | 34.55 | 17.06 | 8.12 | 3.51 |
| $MgO$ | 0 | 0 | 0 | 0.01 | 0 | 0.13 | 0.13 | 0.13 | 0.09 | 0 | 0 |
| $Ce_2O_3$ | 0.07 | 0.03 | 0.08 | 0 | 0.02 | 0.06 | 0.08 | 0 | 0 | 0 | 0 |
| $ThO_2$ | 0.01 | 0 | 0.01 | 0 | 0.01 | 0.04 | 0 | 0 | 0 | 0 | 0 |
| $Al_2O_3$ | 0.01 | 0 | 0.02 | 0 | 0.03 | 0.01 | 1.38 | 0.02 | 0.05 | 0.01 | 0.01 |
| $Nd_2O_3$ | 0.02 | 0 | 0 | 0 | 0.06 | 0.02 | 0 | 0 | 0.02 | 0 | 0 |
| $UO_2$ | 0 | 0 | 0.01 | 0.01 | 0 | 0.03 | 0 | 0.01 | 0.02 | 0 | 0 |
| $Gd_2O_3$ | 0 | 0 | 0 | 0 | 0 | 0 | 0 | 0 | 0 | 0 | 0 |
| $CaO$ | 0.02 | 0 | 0.02 | 0 | 0.01 | 0 | 0.75 | 0.03 | 0 | 0 | 0.01 |
| $Dy_2O_3$ | 0 | 4.95 | 0.03 | 5.05 | 0.04 | 5.01 | 3.23 | 4.49 | 3.79 | 0.01 | 0.01 |
| $BaO$ | 0.31 | 0.15 | 0.25 | 0.13 | 0.37 | 0.12 | 0.11 | 0.14 | 0.39 | 0.20 | 0.44 |
| $Yb_2O_3$ | 0 | 0.02 | 0.07 | 0 | 0 | 0 | 0 | 0.02 | 0.03 | 0.05 | 0.02 |
| $MnO$ | 0 | 14.03 | 0.13 | 13.09 | 0.01 | 13.06 | 10.10 | 13.10 | 11.75 | 0.01 | 0.02 |
| $TiO_2$ | 94.95 | 49.61 | 84.70 | 48.48 | 87.43 | 51.81 | 53.29 | 30.02 | 40.21 | 87.62 | 94.12 |
| $FeO$ | 1.22 | 30.13 | 4.27 | 28.97 | 3.52 | 33.12 | 25.83 | 18.00 | 27.31 | 3.59 | 1.57 |
| Total | 99.50 | 100.74 | 99.99 | 99.34 | 99.654 | 99.77 | 99.72 | 100.16 | 100.69 | 99.88 | 99.84 |

*Table 3*

Chemical composition of niobian rutile I: sample Dt39, area 2, points 14–17 and points 24–26; sample 2006/13, points 1, 2, 10

| Oxides% | 14 | 15 | 16 | 17 | 24 | 25 | 26 | 1 | 2 | 10 |
|---|---|---|---|---|---|---|---|---|---|---|
| $Ta_2O_5$ | 0 | 0 | 0.12 | 0.01 | 0 | 0 | 0 | 0 | 0 | 0 |
| $ZrO_2$ | 0 | 0.02 | 0 | 0.02 | 0 | 0 | 0 | 0 | 0 | 0 |
| $La_2O_3$ | 0 | 0 | 0 | 0.04 | 0 | 0 | 0 | 0.01 | 0 | 0 |
| $Nb_2O_5$ | 8.9 | 11.30 | 9.57 | 10.85 | 6.12 | 3.34 | 8.80 | 2.81 | 9.34 | 2.39 |
| $Ce_2O_3$ | 0 | 0 | 0.02 | 0.03 | 0 | 0.09 | 0 | 0.07 | 0 | 0.05 |
| $ThO_2$ | 0.02 | 0 | 0.01 | 0 | 0 | 0.025 | 0 | 0.01 | 0 | 0 |
| $Gd_2O_3$ | 0.02 | 0 | 0.02 | 0 | 0.023 | 0 | 0 | 0 | 0 | 0.04 |
| $CaO$ | 0.01 | 0 | 0.01 | 0.01 | 0.085 | 0.02 | 0.01 | 0.025 | 0.05 | 0.01 |
| $MgO$ | 0 | 0 | 0 | 0 | 0 | 0 | 0 | 0 | 0 | 0 |

*Table 3*

(continued)

| Oxides% | 14 | 15 | 16 | 17 | 24 | 25 | 26 | 1 | 2 | 10 |
|---|---|---|---|---|---|---|---|---|---|---|
| $Al_2O_3$ | 0.06 | 0.09 | 0.09 | 0.08 | 0.081 | 0.05 | 0.06 | 0.02 | 0.02 | 0 |
| $Nd_2O_3$ | 0.03 | 0 | 0.01 | 0.03 | 0.022 | 0 | 0 | 0.02 | 0 | 0 |
| $Dy_2O_3$ | 0 | 0 | 0 | 0 | 0.039 | 0.05 | 0 | 0 | 0.03 | 0.05 |
| $Yb_2O_3$ | 0.01 | 0.01 | 0 | 0 | 0 | 0 | 0 | 0.05 | 0 | 0 |
| MnO | 0 | 0.01 | 0.04 | 0 | 0.008 | 0 | 0.01 | 0 | 0.01 | 0.01 |
| FeO | 9.75 | 10.84 | 9.35 | 10.09 | 8.467 | 4.73 | 10.00 | 1.22 | 4.27 | 1.17 |
| $TiO_2$ | 88.27 | 80.00 | 81.52 | 80.00 | 90.671 | 93.872 | 81.04 | 94.96 | 84.69 | 96.09 |
| Total | 99.18 | 100.18 | 100.60 | 100.94 | 105.549 | 100.17 | 100.97 | 99.51 | 99.03 | 99.03 |

*Table 3A*

Sample DT2006-13, points 1, 2, 10, 13, 18, 23, 24

| Oxides | 1 | 2 | 10 | 13 | 18 | 23 | 24 |
|---|---|---|---|---|---|---|---|
| $Ta_2O_5$ | 0 | 0 | 0 | 0.06 | 0.011 | 0 | 0 |
| $ZrO_2$ | 0 | 0 | 0 | 0 | 0 | 0.02 | 0.01 |
| $La_2O_3$ | 0.01 | 0 | 0 | 0 | 0 | 0.022 | 0 |
| $Nb_2O_5$ | 2.81 | 9.34 | 2.39 | 8.03 | 1.35 | 8.12 | 3.51 |
| $Ce_2O_3$ | 0.07 | 0 | 0.05 | 0.02 | 0 | 0 | 0.08 |
| $ThO_2$ | 0.01 | 0 | 0.01 | 0.02 | 0 | 0 | 0 |
| $Gd_2O_3$ | 0 | 0 | 0.05 | 0.01 | 0.01 | 0 | 0 |
| CaO | 0.02 | 0.02 | 0.01 | 0.01 | 0.01 | 0.01 | 0.01 |
| MgO | 0 | 0 | 0 | 0.06 | 0 | 0 | 0 |
| BaO | 0.31 | 0.25 | 0.36 | 0.37 | 0.49 | 0.39 | 0.44 |
| $Al_2O_3$ | 0.02 | 0.02 | 0.01 | 0.04 | 0.01 | 0.01 | 0.01 |
| $Nd_2O_3$ | 0.02 | 0 | 0 | 0.06 | 0.04 | 0.01 | 0 |
| $Dy_2O_3$ | 0 | 0.03 | 0.05 | 0.04 | 0 | 0.01 | 0.01 |
| $Yb_2O_3$ | 0.05 | 0 | 0 | 0 | 0 | 0.05 | 0.03 |
| MnO | 0.01 | 0.01 | 0.01 | 0.01 | 0 | 0.01 | 0.02 |
| FeO | 1.22 | 4.27 | 1.17 | 3.52 | 0.75 | 3.59 | 1.58 |
| $TiO_2$ | 94.95 | 84.69 | 96.09 | 87.43 | 97.73 | 87.63 | 94.12 |
| Total | 99.51 | 99.03 | 100.24 | 99.65 | 100.40 | 99.88 | 99.84 |

*Table 3B*

Sample DT214R/ 25-26, 29-31, 33, 35

| Oxides Point | FeO | $TiO_2$ | $Nb_2O_5$ | $SiO_2$ | MgO | $Ta_2O_5$ | MnO | Total |
|---|---|---|---|---|---|---|---|---|
| 25 | 3.74 | 84.83 | 9.44 | 0 | 0 | 0 | 0.01 | 98.02 |
| 26 | 3.53 | 84.90 | 9.48 | 0.03 | 0 | 0.22 | 0 | 98.16 |
| 29 | 3.33 | 86.48 | 8.44 | 0 | 0 | 0.24 | 0.03 | 98.49 |
| 30 | 2.86 | 87.41 | 7.69 | 0 | 0 | 0.17 | 0 | 98.12 |
| 31 | 2.82 | 87.99 | 7.15 | 0 | 0 | 0 | 0.10 | 98.05 |
| 33 | 2.61 | 90.27 | 6.23 | 0.01 | 0.05 | 0.18 | 0.06 | 99.40 |
| 35 | 2.05 | 91.17 | 5.04 | 0 | 0 | 0 | 0.04 | 98.31 |

**Ilmenite**, $FeTiO_3$, forms a series with Mn-ilmenite and pyrophanite. It occurs in big grains as intergrowth with niobian rutile (Fig. 3). Also, it forms veins in niobian rutile, being later than it. The ilmenite in these intergrowths has less/no Nb than niobian rutile (Table 2). It has low MgO content, but more than in niobian rutile. Also, the MnO content is higher in ilmenite than in niobian rutile. Sometimes, the MnO content could be higher than FeO one. The Jolotca ilmenite has a variable composition, from pure ilmenite term to manganese ilmenite and pyrophanite ($MnTiO_3$). The **Mn-ilmenite** occurs as veins in niobian rutile

(Figs. 4 right and left). Also, the Mn-ilmenite can occurs as fine lamellae oriented within the host rutile (exsolutions/intergrwths in/with niobian rutile) as it can see in many back scattered electronic images (Fig. 10 right image and Fig. 11 left). In the optical image, made in transmitted light, the later Mn ilmenite substituts marginal and through little veins the niobian rutile (Fig. 12 left). In Fig. 12 right, one can see groups of brown acicular crystals (Mn-ilmenite?), crossing at $60^0$, enclosed in niobian rutile. Mn ilmenite has $TiO_2 = 52.75$, $FeO = 40.25$ and $MnO = 6.99$, in sample Dt37/2. Ilmenite is typically intergrown

with niobian rutile and the latter has mangancolumbite /ferrocolumbite (Figs. 9, 10, 11) and euxenite-(Y) exsolutions. Some little red grains of mm size with pyrophanite compositions were determined in sample 2006/13, in association with a fibrous Ba pink mica, probably a kinohistalite (?) and barite, probably formed later, as secondary minerals.



Fig 12. Nb-rutile (brownish yellow) substituted/intergrowth by/with niobian Mn-ilmenite (black), sample Dt2006/13 (left); unmixed Mn-ilmenite (?) (brown) in niobian rutile (greenish yellow), sampleBel/l3A (right photo).

*Table 4*

Chemical composition of rich niobian rutile, rutile II (old name manganoan "ilmenorutile")
Sample DT2006/13, points 15, 16, 17, 20

| Oxides % | 15 | 16 | 17 | 20 |
|---|---|---|---|---|
| $Nb_2O_5$ | 24.69 | 37.25 | 31.39 | 17.0 |
| CaO | 0.75 | 0.03 | 0.01 | 0 |
| MgO | 0.14 | 0.13 | 0.09 | 0.09 |
| $Dy_2O_3$ | 3.23 | 4.49 | 4.07 | 3.79 |
| MnO | 14.11 | 14.10 | 12.10 | 12.79 |
| FeO | 20.93 | 20.99 | 20.06 | 28.31 |
| $TiO_2$ | 35.30 | 32.99 | 32.63 | 41.21 |
| Total | 99.04 | 100.10 | 100.35 | 99.31 |

**Niobian rutile II, rich niobian rutile** (old name manganoan "ilmenorutile" or niobian pyrophanite), is a Ti-Nb-Fe-Mn oxide. It shows no compositional zoning (Fig. 10 left), such as that shown by niobian rutile I, and could be defined as a distinct mineral. It formed during the Nb enrichment solid solutions. Its microprobe chemical composition can be seen in Table 4. It has no $Ta_2O_5$. The $Nb_2O_5$ content of rich Nb-rutile II varies between 17.0–37.55wt%, the FeO and MnO contents of rutile niobian II are higher than that of niobian rutile I. Also, the MnO content of niobian rutile II is higher than that of niobian rutile I.

The niobian rutile is a relatively widespread mineral in the world. It is found in mineralized miaskites and metasomatic deposits associated with plumassitic nepheline syenite; in anorogenic alkaline rare-elements granites and associated metasomatites, and vein deposits; in anorogenic rare-element pegmatites; in peraluminous, orogenic to post-orogenic rare-element granites; and in granitic rare-element pegmatites of orogenic affiliation. But, the big growing and oscillatory zoning have not been seen in these occurrences such as Jolotca. Its occurrence could be linked with the alkaline/carbonatite (?) phase of the alkaline intrusive Ditrău complex; the presence of $Cr_2O_3$ in its composition suggests its mantle origin. The Jolotca niobian rutile is associated with rutile (grown on it), ferrocolumbite, manganocolumbite, chevkinite-(Ce), monazite-(Ce), allanite-(Ce), pyrite, sphalerite, phlogopite, natrolite, calcite in the Jolotca area. In the Belcina area the niobian rutile, less frequent, is associated with thorite, thorogummite, xenotime-(Y), goethite, hematite,

aegirine, riebeckite, late zircon, molybdenite in calcite-ankerite rocks, being the oldest mineral (Hirtopanu *et al.*, 2013b).

## THE MINERAL ASSOCIATIONS OF NIOBIAN RUTILE

Except the **ilmenite** that was described above, and with which it is closely associated, the niobian rutile has unmixings of **columbites, euxenites** and **aeschynites.**

### Columbite Group

The orthorhombic ferrocolumbite $(Fe,Mn)Nb_2O_6$ and mangancolumbite $(Mn,Fe)Nb_2O$ minerals have a general formula $AM_2O_6$, where A = Fe, Mn, Mg and M = Nb, Ta. Minor quantities of $Fe^{3+}$, Sc, Ti, Sn and W are commonly present (Černý and Ercit, 1985). End-member compositions include: ferrocolumbite $(FeNb_2O_6)$, manganocolumbite $(MnNb_2O_6)$, magnocolumbite $(MgNb_2O_6)$, mangano- tantalite $(MnTa_2O_6)$ and ferrotantalite $(FeTa_2O_6)$. The end term ferrotantalite- belongs to the tetragonal tapiolite series. The columbites-tantalites are decidedly the most widespread of the all Nb, Ta-bearing minerals, found in substantial quantities in most types of deposits. In Jolotca area, generally the columbites occur as a exsolved phase, from a primary solid solutions with niobian rutile. However, some mangancolumbite grains occur apparently without any link with niobian rutile (Fig. 13). The metamictization of columbites occurs in the presence of U and Th, especially in the Belcina area (Hirtopanu *et al.*, 2013b) while in Jolotca area they are clean crystals (Fig. 13).

The composition of columbites is much more restricted to the Nb and Fe-rich, but the Mn columbite is widespread. The manganocolumbites have short prismatic or equal grains and form groups or aggregates of subparallel-radiating crystals of a few mm (Fig. 13, optical image and its BSE image) They have a distinct cleavage on (100) and less distinct on (010). In transmitted light they are red to brown, brown-black colour. The cleavages and the biaxial optical character differentiate them from the pyrochlores of the same colour. In transmitted light the manganocolumbite has a light red colour, while the ferrocolumbite has a dark red to black colour. Sometimes, ferrocolumbite is opaque, especially when the FeO content is too high. The chemical composition of ferrocolumbite is presented in Table 5 and of mangancolumbite in Table 6 (Hirtopanu *et al.*, 2010a).
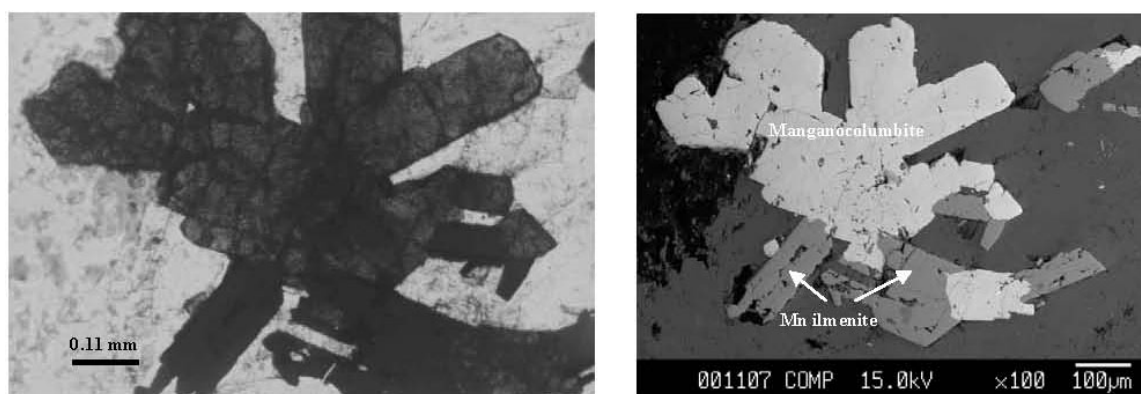


Fig. 13. Mangancolumbite (red prisms), Mn ilmenite (black prisms), transmitted light, NII (left) and its BSE image (right): manganocolumbite (white), Mn-ilmenite (grey), sample Dt2016/13; see its chemical analyses in Table 6.

*Table 5*

The chemical composition of ferrocolumbite, samples BEL12/1-9; BEL10A/1A; see its BSE image in Figure 11 right

| Oxides% | 1 | 2 | 3 | 4 | 5 | 6 | 7 | 8 | 9 | 1A |
|---|---|---|---|---|---|---|---|---|---|---|
| $Nb_2O_5$ | 73.56 | 71.53 | 73.43 | 71.33 | 73.90 | 73.07 | 73.12 | 73.80 | 71.43 | 75.42 |
| $Ta_2O_5$ | 0 | 0 | 0 | 0 | 0 | 0.25 | 0 | 0 | 0 | 0 |
| MnO | 7.83 | 8.17 | 6.03 | 8.17 | 6.58 | 8.52 | 9.64 | 5.66 | 8.26 | 2.01 |
| FeO | 16.09 | 16.58 | 17.36 | 16.63 | 16.16 | 15.73 | 14.83 | 16.77 | 16.11 | 19.26 |
| MgO | 0.43 | 0 | 0.46 | 0.39 | 0.42 | 0.52 | 0.51 | 0.06 | 0.25 | 0 |
| $TiO_2$ | 2.21 | 2.19 | 2.59 | 2.15 | 2.61 | 2.30 | 2.28 | 3.15 | 3.54 | 3.08 |
| Total | 100.11 | 98.49 | 99.87 | 98.67 | 99.67 | 100.41 | 100.39 | 99.45 | 99.60 | 99.77 |

The chemical composition of manganocolumbite, samples 2006-13/1, 3, 8, 9, 11, 12; DT2/33;
see its BSE image in Figure11 left

| Oxides % | 1 | 3 | 8 | 9 | 11 | 12 | 33 |
|---|---|---|---|---|---|---|---|
| $Nb_2O_5$ | 76.96 | 69.80 | 77.46 | 78.28 | 76.30 | 77.07 | 76.28 |
| $TiO_2$ | 3.30 | 7.99 | 2.62 | 2.39 | 2.00 | 2.66 | 2.80 |
| CaO | 0.96 | 1.09 | 1.36 | 0.03 | 0.12 | 1.39 | 0.04 |
| MnO | 11.36 | 13.13 | 11.38 | 12.27 | 13.04 | 11.00 | 14.9 |
| FeO | 6.82 | 7.17 | 6.82 | 7.10 | 6.59 | 7.16 | 4.44 |
| Total | 99.40 | 99.07 | 99.65 | 100.09 | 100.06 | 99.28 | 99.59 |

As one can see in Tables 5 and 6 (Hirtopanu *et al.*, 2010a), the $Fe_2O_3$ (present especially in yttrocolumbite), the $WO_3$, $ThO_2$, $ZrO_2$, $Ce_2O_3$, Mg and $SnO_2$ contents were not determined. These elements were determined in others niobian rutile in the world, and they could be present in Jolotca columbites. The columbites are associated with Nb-Ti-Fe minerals (niobian rutile, ilmenite, manganoan niobian rutile, and pyrophanite) as exsolution products. In the BSE images in Figs. 9, 10 and 11 (right image), one can see the latest ferrocolumbite grains (white) and ilmenite (white grey) substituting the niobian rutile. It seems that the niobian rutile is older than ilmenite and of course older than columbites.

**Yttrocolumbite** (Y,U,Fe,Mn)(Nb,Ta)$O_4$ (orthorhombic) is less spread than Fe-Mn columbites. It was determined with the microprobe in sample Dt2006/13 point 22, and has informative representative qualitative composition: $Y_2O_3 = 12.34$, $La_2O_3 = 0.01$, $Nb_2O_5 = 48.28$, $Ce_2O_3 = 2.08$, $Nd_2O_3 = 7.65$, $UO_2 = 0.06$, $Gd_2O_3 = 8.06$, CaO $= 0.31$, $Dy_2O_3 = 5.61$, $Yb_2O_3 = 0.02$, $TiO_2 = 0.72$, FeO $= 1.01$.

### Euxenites group

**Euxenite-(Y)**, (Y,Ca,Ce,U,Th)(Nb,Ta,Ti)$_2O_6$, orthorhombic, typically metamictic. It occurs in close association with columbites as exsolutions in the Nb-rutile-ilmenite intergrowth. Also, it was determined, as independent grains, in close association with red sphalerite (Fig. 14). The euxenites have a general formula of $AM_2O_6$ and an ordered columbite type structure (Černý and Ercit, 1989). Octahedral position A is occupied by Y, REE, Ca U and Th, while tetrahedral position M is occupied by Ti, Nb and Ta. In contrast to the columbite tantalite group senso stricto, the A cations in euxenites are much larger and coordinated with eight cations (Černý and Ercit,

1989). These last authors consider that the principal modes of chemical substitution are (Ca+Nb,Ta)↔(Y,REE) and Ca+(U,Th) ↔ 2(Y,REE), the first one introducing substantial quantities of a fersmitelike component. The euxenites from Jolotca form isometric subhedral to euhedral grains usually elongated from short prisms to needle-shaped crystals. In transmitted light the prismatic crystals have a brown, green, green-yellow to light greenish yellow and brown colour (Fig. 14), being similar to pyrochlore at first sight, because they are of the same colour. Their refringence is high, around/more than 2. Analysed with the microprobe, they have a Y,HREE-dominant composition. The main oxide compounds of euxenite-(Y) show the following variation (%wt): $TiO_2 = 21.33–32.75$, $Nb_2O_5 = 40.16–44.99$, $Y_2O_3 = 14.45–22.15$, CaO $= 0.98–1.69$, $ThO_2 = 0.58–2.66$ (sample Dt6, points 1,2 and Dt39, point 27). In sample Dt39 were also determined $Nd_2O_3 = 4.35$, $Gd_2O_3 = 4.24$, $Dy_2O_3 = 3.49$ and $Yb_2O_3 = 0.72$ (%wt). Generally, euxenites occur frequently as a segregation earlier product, probably prior to columbites and aeshynites, from the rutile niobian-ilmenite intergrowth mixed precursor.

**Polycrase-(Y)**, Y(Ti,Nb,Ta)$_2$(O,OH)$_6$, orthorhombic, commonly metamictic, because of its Th and U contents. Under the microscope it has a short to long prismatic crystals of a few mm, striated parallel to elongation, forming parallel to radiating aggregates. In transmitted light it shows a brown to yellow brown colour and it is isotropic because of metamictization. The polycrase-(Y) and the euxenite-(Y) occur as accessory minerals. The difference between polycrase-(Y) and euxenite-(Y) is their $TiO_2$ and $Nb_2O_5$ contents. In euxenite-(Y) $Nb_2O_5>TiO_2$ and in policrase-(Y), $TiO_2>Nb_2O_5$. The old name of polycrase-(Y), yttrocrasite, was discredited by IMA (Peacor *et al.*, 1982). Compositionally, the Ditrău polycrase-(Y) has

(Y,REE>(U,Th)(Ti,Nb,Ta)$_2$O$_6$ as shown by Černý and Ercit, 1989), such as can be seen in Table 8. The main oxide compounds determined in the polycrase-(Y) composition, have the following variations (%wt): Y$_2$O$_3$ = 12.64–20.15, Ta$_2$O$_5$ = 0–0.07, Nb$_2$O$_5$ = 7.14–10.69, La$_2$O$_3$ = –0.52, Ce$_2$O$_3$ = 2.67–8.81, Gd$_2$O$_3$=3.87–4–67, Nd$_2$O$_3$ =5.71–17.37, Dy$_2$O$_3$ = 1.67–3.56, Yb$_2$O$_3$ = 0.15–0.49, TiO$_2$ = 39.66–44.42, CaO = 0.27–0.63, ThO$_2$ = 0.36–2.16, FeO = 2.03–4.05 (sample TDT). The REE content of the polycrase-(Y) is commonly dominated by Y group, showing enrichment in Gd and Dy. Among the LREE, the polycrase-(Y) has enrichment in Nd$_2$O$_3$ over Ce$_2$O$_3$. Both euxenites are at least partially altered to Ca-containing pyrochlore, during the last stage of mineralizing process.
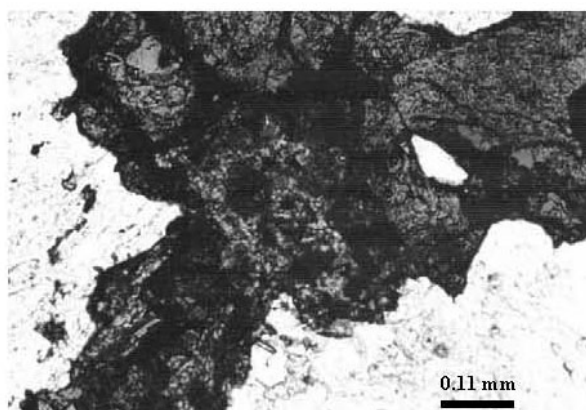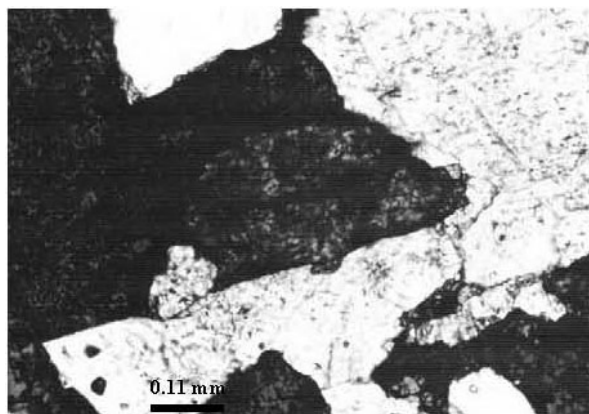


Fig. 14. Euxenite-(Y), (yellow brown, green, partially metamictic), sphalerite (red), calcite (white greenish), NII, sample Dt6A (left photo); euxenite-(Y) (yellowish green, partially metamictic), sphalerite (red), calcite (white, very light green), NII, sample Dt6/2 (right photo).

### Aeshynites group

**Aeshynite-(Ce)**,(Ce,Ca,Fe,Th)(Ti,Nb)$_2$(O,OH)$_6$ and **aechynite-**(Nd), (Nd,Ce,Ca)(Ti,Nb)$_2$(O,OH)$_6$ were described previously in Ditrau occurrence (Hirtopanu *et al.*, 2010a). Both aeshynites occur closely associated with Nb-Ti-Fe-Mn oxide minerals. The textural relation among niobian rutile and both aechynites, one can see in the Figure 15, where the niobian rutile appears as relics in aeshynites. Some rutile grains which cut through the cleavages of aeshynite (Fig. 15A), probably belong to a new rutile generation, formed after aechynites.
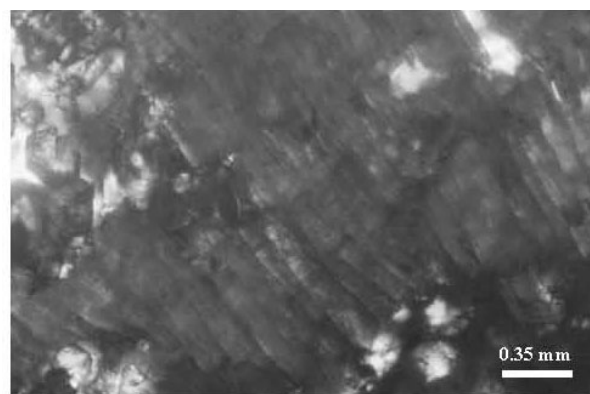


Fig. 15B. Relics of Nb-rutile (yellow black) in aeshynite-(Nd)(red), (15A); Nb rutile (yellow brown black) relics in aeshynite-(Ce)(yellow red), sample Dt39.

The aechynites occur as exsolutions in ilmenite-niobian rutile intergrowth, being probably an ummixed product from an old common precursor, originated in upper mantle.

### GENETICAL REMARKS

We can make only some genetical remarks on Joloca niobian rutile, by comparing it with the niobian rutile from other occurrences. Having very low Ta content, the niobian rutile, does not seem to



Fig. 15A

be characteristic of alkali intrusive rocks, being similar with that intergrown niobian rutile/ilmenite, reported in a number of kimberlite localities in recent years. High pressure Nb-Cr-rutile in the Orapa kimberlite, Botswana, containing lamellar ilmenite, is considered to result from an exsolution-like process with strong partitioning of Nb+Zr in rutile and Mg in ilmenite, and with Cr selectively partitioned to a lesser degree in rutile (Tollo & Haggerty, 1987). The chemically distinguishing features between kimberlitic Nb rutile and that present in the Jolotca, occurring in alkaline suites, are high Cr content and the presence of Zr in a kimberlite one. The same low Ta concentration in kimberlitic Nb rutile is also characteristic of Jolotca Nb-rutile. Also, the Jolotca Nb rutile, such as the kimberlite Nb rutile, has some Cr content (1.478 %wt maximum), but not so high as kimberlitic Nb-rutile (8.2 %wt maximum). The values of $Nb_2O_3$ in Jolotca niobian I is similar with some of that from Orapa niobian rutile. But, the values of $Nb_2O_5$ in Jolotca Nb-rutile II are higher (up to 33 %wt) than that of kimberlitic Nb rutile (up to 20.9 %wt maximum). Tollo & Haggerty (1987) consider that crystallographic shear-based structures related to α-PbO2 are the most probable progenitors to accommodate the extraordinarily large concentrations of Nb, Cr, Zr and Fe at the P-T conditions of the upper mantle.

## CONCLUSIONS

The Jolotca niobian rutile from Ditrau alkaline intrusive complex displays exsolution textures. The iron, manganese and manganese+iron columbites, yttrocolumbite, are also products of exsolution from a niobian rutile+ilmenite intergrowth. Among the exsolutions products, both aechynites show large development. Also, many microscopic euxenite grains were determined as exsolutions in niobian rutile. The intergrowths of Nb rutile+ilmenite indicate that they were formed from a homogeneous solid solutions that had existed at higher temperatures and pressures. However, the textural relations of the two minerals, show that niobian rutile is the oldest mineral. The two generations of niobian rutile formed in different stages, were differentiated by chemical composition, specially by $Nb_2O_5$ content: niobian rutile I has lower $Nb_2O_5$ content than niobian rich rutile II. The chemically distinguishing features of Jolotca niobian rutile are very low Ta and some $Cr_2O_3$ (up

to 1.45) indicating its origin from complex alkaline-carbonatite (?) sources. Also, the values for $Nb_2O_5$ in rich niobian rutile II are higher than any previously recorded for niobian rutile from alkaline suites. So, some $Cr_2O_3$ and very small $ZrO_2$ contents of niobian rutile, and also some MgO content in ilmenite, could be good evidence of their common origin from upper mantle (Tollo & Haggerty, 1987), in high-pressure regimes, from the most probable progenitors that accommodated large concentrations of Nb, Fe, Mn and less Cr, Mg, Zr.

## REFERENCES

1. Burke, A.J.E., 2006, A mass discreditation of GQN minerals, 2006, The Canadian Mineralogist, v.44, p.1557-60.
2. Černý, P. & Ercit, T. S. 1989: Mineralogy of niobium and tantalum: Crystal chemical relationships, paragenetic aspects and their economic implications. In Moller, P., Cerny, P. & Saupé, F. (eds.) Lanthanides, Tantalum and Niobium, Berlin: Springer Verlag. p. 27–79.
3. Černý, P., R. Chapman, W. B. Simmons, and L.E. Chackowsky (1999), Niobian rutil from Mc Guire, Solid solutions, exsolution and oxidation, American Mineralogist, vol.84, p. 754-763.
4. Černý, P. M., Novak, R., Chapman, K. J. Ferriera, 2007, Subsolidus behavior of niobian rutile from Pisek Czech Republic: a model for exsolution in W- and $Fe^{2+}$ rich phases, Journal of Geosciences, vol 52, p. 143-159.
5. Constantinescu, E.1999, Mineralogy in the system of the Earth, London: Imperial College Press. 384 p.
6. Hirtopanu, P., J.C. Andersen & R. J. Fairhurst, 2010a,: Nb, Ta, REE(Y), Ti, Zr, Th, U and Te rare element within the Ditrau alkaline intrusive complex, Eastern Carpathians, Romania, Mineralogy of Szekelyland, Eastern Transylvania, Romania, 2010a, Edited by Sandor Szakall and Ferenc Kristaly, Tg. Mures, p. 89-128.
7. Hirtopanu P., Andersen C. Jens & Fairhurst J. Robert, 2010b, Nb, Ta, REE(Y), Ti, Zr, Th, U and Te rare

element minerals within the Ditrău alkaline intrusive complex, East Carpathians, Romania, 20th General Meeting oh the International Mineralogical Association (IMA), 21-27 August 2010, Budapesta, Hungary, CD Abstracts, p. 570.

8.  Hirtopanu, P., C. J. Andersen, J. R. Fairhurst and G. Jakab, 2013a, Allanite-(Ce) and its associations from the Ditrau alkaline intrusive massif, East Carpathians, Romania, 2013a, Proc. Rom. Acad., Series B, 2013, 15(1), p. 59-74.

9.  Hirtopanu P., G. Jakab, C. J. Andersen and J. R., Fairhurst, Thorite, thorogummite and xenotime-(Y) occurrence in Ditrau alkaline intrusive massif, East Carpathians, Romania, 2013b, Proc. Rom. Acad., Series B, 2013, 15(2), p. 111-132.

10. Jakab, Gy., 1998, Geologia masivului alcalin de la Ditrău. Miercurea Ciuc: Ed. Pallas-Akademia. 297 p.

11. Jakab, Gy., 2014, Geneza masivului alcalin Ditrau si zestrea sa minerala, manuscript.

12. Krautner H., Bindea G. (1995), The Ditrau alkaline intrusive complex and its geological environment. Rom.J. Min, 77, supp 3, p. 44, Bucuresti.

13. Molnar P., E., 2000, Hornblendites anddiorites of the Ditro syenite massif, 172p., Szeged, Hungary.

14. Pasteris, J.D. (1980), The significance of groundmass ilmenite and megacryst ilmenite in kimberlites. Contr.Mineral.Petrology 75, p. 315-325.

15. Peacor, D. R., Simmons, W.B., Essene J.E., and Heinrich, W.E., 1982, New data on and discreditation of „texasite", „albrittonite", „cuproartiniter", „cuprohydro-magnesite" and „yttromicrolite", with corrected data on nickelbischofite, rowlandite, and yttrocrasite, 1982, Am. Mineral., v.67, p. 156-169.

16. Tollo R.P., & Haggerty S.E., 1987, Nb-Cr rutile in the Orapa kimberlite, Botswana, Canadian Mineralogist, vol. 25, p. 251-264.